A neutron diffraction and Mössbauer spectral study of the magnetic spin reorientation in $Nd_6Fe_{13}Si$

2002 J. Phys.: Condens. Matter 14 12391

(http://iopscience.iop.org/0953-8984/14/47/313)

INSTITUTE OF PHYSICS PUBLISHING JOURNAL OF PHYSICS: CONDENSED MATTER

J. Phys.: Condens. Matter **14** (2002) 12391–12409 PII: S0953-8984(02)39916-8

A neutron diffraction and Mössbauer spectral study of the magnetic spin reorientation in $Nd_6Fe_{13}Si$

Olivier Isnard[1], Gary J Long[2], Dimitri Hautot[2], K H J Buschow[3] and Fernande Grandjean[4]

[1] Laboratoire de Cristallographie du CNRS, Associé à l'Université J Fourier et à l'INPG, CNRS, F-38042 Grenoble, France
[2] Department of Chemistry, University of Missouri-Rolla, Rolla, MO 65409-0010, USA
[3] Van der Waals-Zeeman Institute, University of Amsterdam, Valckenierstraat, 65, NL-1018 XE Amsterdam, The Netherlands
[4] Institut de Physique, B5, Université de Liège, B-4000 Sart-Tilman, Belgium

E-mail: isnard@labs.polycnrs-gre.fr, glong@umr.edu, buschow@phys.uva.nl and fgrandjean@ulg.ac.be

Received 24 July 2002
Published 15 November 2002
Online at stacks.iop.org/JPhysCM/14/12391

Abstract

Powder neutron diffraction and Mössbauer spectral studies have been carried out on $Nd_6Fe_{13}Si$ between 2–295 K. The nuclear neutron scattering shows that $Nd_6Fe_{13}Si$ has the tetragonal $I4/mcm$ crystal structure at all temperatures. A collinear antiferromagnetic structure with the wavevector $q = (0, 0, 1)$ is observed below the Néel temperature of 421 K. A spin reorientation is observed at ∼100 K in both the neutron diffraction patterns and the Mössbauer spectra. Above and below 100 K, the magnetic moments of the four iron and the two neodymium crystallographic sites are ferromagnetically coupled within one block along the c axis and the resulting magnetic moment of this block is antiferromagnetically coupled with that of the adjacent block along the c axis through a layer of silicon atoms. Above and below 100 K, the magnetic moments are found to be parallel or very close to the c axis and within or close to the (a, b) basal plane of the tetragonal unit cell, respectively. This first-order spontaneous zero-field spin reorientation occurs cooperatively and involves both the neodymium and iron magnetic moments. The powder neutron diffraction between 10 and 200 K indicates anisotropic lattice changes associated with a change in the magnetoelastic coupling in this compound. The Mössbauer spectral hyperfine parameters are those expected for axial and basal magnetization directions in $Nd_6Fe_{13}Si$ and further indicate the existence of a 75% basal and 25% axial mixed magnetic phase even at 4.2 K, a mixed magnetic phase which results from the influence of the secondary ferromagnetic Nd_2Fe_{17} phase on the primary $Nd_6Fe_{13}Si$ phase.

1. Introduction

Over the past several years there have been many studies devoted to rare-earth transition-metal, R–M, compounds which contain silicon. Some of these silicon compounds are pseudobinary compounds, such as the $R_2M_{17-x}Si_x$ and $RM_{12-x}Si_x$ compounds [1–5], and some are true ternary compounds, such as $Nd_6Fe_{13}Si$, in which silicon [6] is required to stabilize the crystal structure. Further, special attention has been devoted to some iron-rich compounds, such as $Nd_2Fe_{14}B$, that are potential hard magnetic materials. Because the $Nd_6Fe_{13}X$ compounds [7–9], where X is Si, Al, Ga, Cu, Ge, Ag, Au, Sn or Sb, sometimes appear between the grains of $Nd_2Fe_{14}B$ in hard magnetic materials [6, 10], the study of their structural and magnetic properties has practical importance. The crystallization of the $Nd_6Fe_{13}X$ compounds sometimes improve the hard magnetic properties of a material through a significant increase in its coercivity [10, 11].

In a Mössbauer spectral study [12] of $Nd_6Fe_{13}Si$ between 80 and 295 K, we observed a spin reorientation at ∼110 K from axial magnetization at higher temperatures to predominantly basal at lower temperatures. This reorientation was observed as a dramatic change in the overall shape of the Mössbauer spectra observed between 135 and 80 K. Above 150 K the spectrum could be nicely fit with an axial model involving four sextets associated with the four crystallographically different iron sites in $Nd_6Fe_{13}Si$. However, at 135 K and below a fit of the observed spectra required the combined use of the four axial sextets and five additional sextets which were associated with the five magnetically inequivalent iron sites expected for a basal orientation of the iron magnetic moments. The relative amount of the axial component decreased gradually between 135 and 80 K such that at 80 K the spectral analysis indicated that the compound was 75% basal and 25% axial.

$Nd_6Fe_{13}Si$ crystallizes in the tetragonal $I4/mcm$ space group number 140, and its structure (see figure 1(a) [6]) consists of a series of blocks or layers stacked along the tetragonal c axis (see figure 1(b)). In $Nd_6Fe_{13}Si$ the layers containing neodymium and iron are separated by layers containing only silicon on the 4a site. The neodymium, which occupies the 8f and 16l sites, is found in layers adjacent to the silicon layer, and the layers of iron 4d, 16k, $16l_1$ and $16l_2$ sites are sandwiched between the neodymium layers.

An antiferromagnetic structure was proposed [13] for $Nd_6Fe_{13}Si$ on the basis of a room temperature neutron diffraction study. In this structure [13], the magnetic moments are parallel or antiparallel to the c axis and the iron 16k and 16l magnetic moments are antiparallel to the remaining moments. Unfortunately, this magnetic structure is inconsistent with the iron-57 Mössbauer spectral hyperfine fields observed [12, 14] in $Nd_6Fe_{13}Si$. Further, recent magnetic [15] and neutron diffraction studies [16, 17] have suggested alternative magnetic structures for several $R_6Fe_{13}X$ compounds with R = Pr or Nd and X = Si, Ag or Au. In these magnetic structures, the magnetic moments within one of the rare-earth transition-metal layers are ferromagnetically coupled and these layers are antiferromagnetically coupled across the layer containing X. These magnetic structural analyses are based on group theory [18] and involve a consideration of all possible magnetic symmetries compatible with the crystal structure [16, 17]. Neutron diffraction studies [16, 17] of $Pr_6Fe_{13}Ag$, $Pr_6Fe_{13}Si$, $Pr_6Fe_{13}Au$ and $Nd_6Fe_{13}Au$ indicate that the magnetic moments in the ferromagnetic layers lie in the basal plane of the tetragonal structure. In contrast, a neutron diffraction study [19] of $Nd_6Fe_{13}Sn$ indicates that the magnetic moments in the ferromagnetic layers are parallel to the c axis at room temperature and are canted by 10° from the c axis at 1.5 K.

Because our earlier Mössbauer spectral study [12] of $Nd_6Fe_{13}Si$ revealed both a room temperature magnetic structure, which was incompatible with that derived from a low resolution neutron diffraction study [13], and a partial spin reorientation below ∼135 K, we

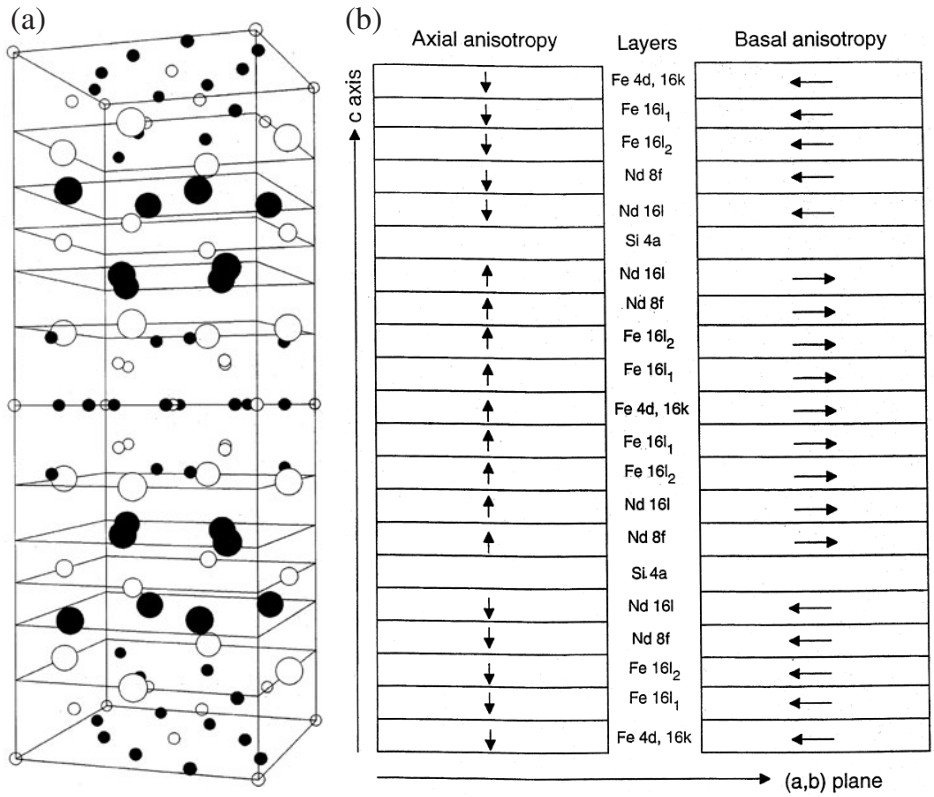

Figure 1. (a) The crystal structure of $Nd_6Fe_{13}Si$ where the large black and white atoms are neodymium 16l and 8f, the intermediate size white atoms are silicon 4a, the small black atoms are iron 16k and $16l_2$ and the small white atoms are iron 4d and $16l_1$. The layers containing the neodymium 8f, neodymium 16l and silicon 4a sites are delineated. (b) A schematic diagram of the magnetic structure of $Nd_6Fe_{13}Si$ at high temperature, left, and low temperature, right.

have carried out additional Mössbauer spectral measurements between 4.2 and 80 K with the initial expectation of observing a complete spin reorientation at 4.2 K. In addition, we have carried out a detailed neutron diffraction study of $Nd_6Fe_{13}Si$ between 2 and 295 K with the goal of determining the temperature dependence of its magnetic structure.

2. Experiment

2.1. Synthesis

The sample of $Nd_6Fe_{13}Si$ studied herein is the sample previously prepared and characterized by x-ray diffraction and magnetic measurements [15]. As indicated by de Groot *et al* [15] it is virtually impossible to synthesize single-phase $Nd_6Fe_{13}Si$, because of the solubility of silicon in Nd_2Fe_{17}. In order to prepare an almost single-phase compound, these authors used an alloy starting composition of $Nd_{6.4}Fe_{13}Si_{1.3}$ and estimated, from the increases in the magnetization and Curie temperature, that approximately 0.5 wt.% of $Nd_2Fe_{16}Si$ was present in $Nd_6Fe_{13}Si$. This would correspond to a final composition of $Nd_{5.98}Fe_{13.015}Si$.

2.2. Mössbauer spectra

The Mössbauer spectra have been obtained between 4.2 and 135 K on a constant acceleration spectrometer which utilized a room temperature rhodium matrix cobalt-57 source and was calibrated at room temperature with α-iron foil. The Mössbauer spectral absorbers, which contained 26–29 mg cm^{-2} of compound, were prepared from pieces of samples pulverized under liquid toluene and sieved to particle diameters of approximately 0.045 mm or smaller. The accuracy of the hyperfine parameters obtained from Lorentzian lineshape fits is estimated to be ± 0.005 mm s^{-1} for the isomer shift, ± 0.05 mm s^{-1} for the quadrupole shift and ± 2 kOe for the hyperfine field.

2.3. Neutron diffraction

Neutron diffraction experiments were carried out at the high flux reactor of the Institut Laue Langevin. The two-axis D1B powder diffractometer used for this work was equipped with a large one-dimensional 400 cell curved detector which recorded the diffraction pattern over a 2θ range of 80°. The neutron wavelength of 2.52 Å was selected by the (002) reflection of a pyrolitic graphite monochromator and the 2θ step was 0.2°. The use of D1B was essential both for recording the (001) Bragg reflection of $Nd_6Fe_{13}Si$ at very low angle and in following its thermal evolution. A detailed study has been performed between 10 and 200 K by recording the entire diffraction pattern every 3 K.

High resolution powder diffraction patterns have been collected at the University of Missouri Research Reactor by using a linear position-sensitive detector and neutrons with a wavelength of 1.4807 Å. The data were collected for ∼12 h at 295 and 17 K over a 2θ range of 5°–105° with a step of 0.05° on ∼0.5 g of finely powdered $Nd_6Fe_{13}Si$ placed in a thin-walled vanadium container which was placed in a closed cycle refrigerator for the 17 K study. The high-resolution diffractometer does not permit studies at low Q values in reciprocal space, whereas the high-flux long wavelength diffractometer does permit studies at very low angles and, hence, low Q values.

All powder neutron diffraction data were analysed using the Rietveld line profile technique [20] implemented with the program FULLPROF. This program permits multiphase and magnetic structure refinement of each of the components present. A pseudo-Voigt type peak shape function was used in the refinements and, in the case of the D1B data, the peak shape was very close to pure Gaussian. For the very low angle Bragg reflections, an asymmetry parameter has been used to mimic the known instrumental asymmetry. The coherent neutron scattering lengths [21] were 4.149, 9.450 and 7.690 fm for Si, Fe and Nd, respectively. A full description of the Rietveld method used in this paper can be found elsewhere [20].

3. Crystal and magnetic structure

The thermal evolution of the (001) Bragg reflection of $Nd_6Fe_{13}Si$ is shown in figure 2 and this evolution unambiguously confirms the change in the magnetic structure proposed [12, 14] on the basis of the earlier Mössbauer spectral study. Indeed, a huge decrease in intensity of the lowest angle Bragg reflection at $2\theta = 6.4°$ is observed upon heating the sample from 10 to 200 K. The thermal evolution of the integrated intensity of this (001) reflection is shown in figure 3. Unpublished x-ray diffraction results [22] indicate that $Nd_6Fe_{13}Si$ retains the tetragonal $I4/mcm$ space group at low temperature. Consequently, the nuclear scattering in the high resolution powder neutron diffraction patterns obtained at 295 and 17 K, and shown in figures 4 and 5, respectively, has been fitted with this space group and the magnetic scattering

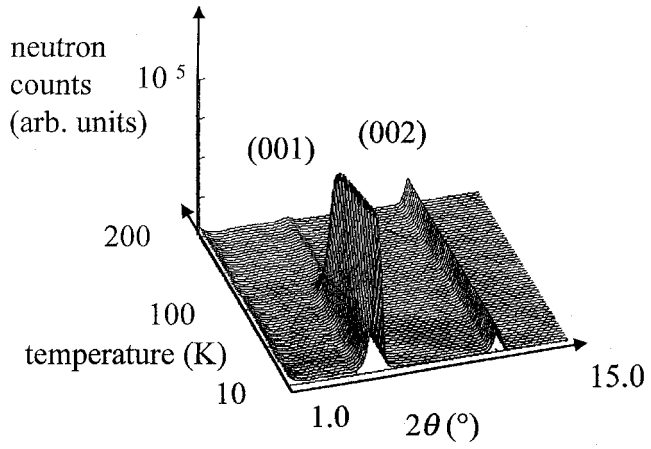

Figure 2. The temperature dependence of the low angle portion of the neutron diffraction pattern of $Nd_6Fe_{13}Si$ obtained on the D1B high flux diffractometer at the ILL.

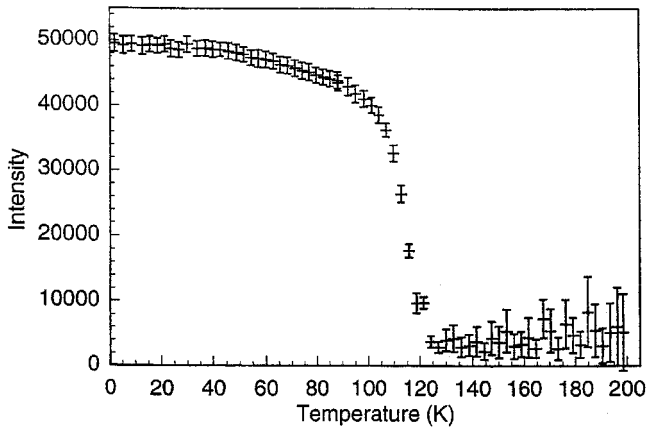

Figure 3. The temperature dependence of the intensity of the (001) magnetic Bragg reflection as determined from the D1B diffractometer data.

has been fitted as described below; the resulting lattice parameters are given in table 1 and the refinement parameters for both the 295 and 17 K high-resolution patterns are given in table 2. The 295 K structural parameters are in excellent agreement with both the single-crystal x-ray results of Allemand *et al* [6] and the x-ray powder diffraction results of de Groot *et al* [15]. In order to minimize the number of refined parameters, only three Debye–Waller factors, one each for neodymium, iron and silicon, were used. In the high resolution neutron diffraction pattern above 2θ angles of 30° there is extensive peak overlap in spite of the high resolution.

In the $I4/mcm$ space group, no nuclear scattering contribution from the crystal structure is possible for the (001) reflection because the I centring requires $h + k + l = 2n$. Consequently, the (001) Bragg reflection must be of magnetic origin and the huge observed change in intensity, see figures 2 and 3, corresponds to a change in magnetic structure at ∼100 K. The presence of the odd (00l) reflections suggests a purely antiferromagnetic structure with the wavevector $q = (0, 0, 1)$. The indexing of the magnetic scattering is permitted by the presence of an antitranslation $(1/2, 1/2, 1/2)$ which in turns leads to a systematic extinction of the magnetic

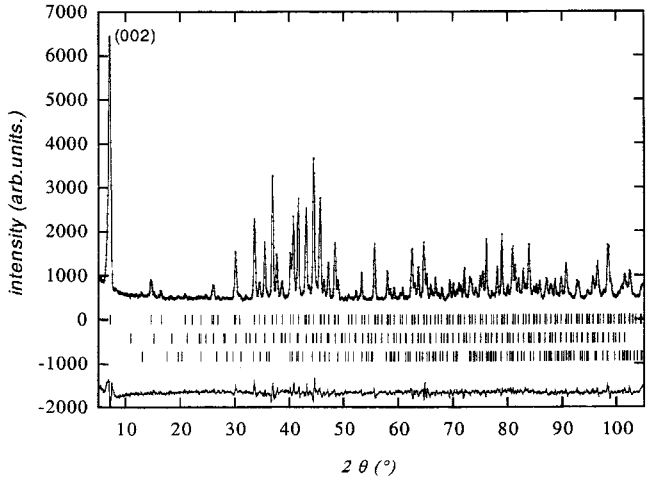

Figure 4. The powder neutron diffraction pattern of $Nd_6Fe_{13}Si$ obtained at 295 K on the MURR high resolution diffractometer with a neutron wavelength of 1.4807 Å. In the upper plot the points represent the experimental data and the full curve is the result of the Rietveld profile analysis. The difference between the experimental data and the calculated pattern is plotted on the same scale in the lowest part of the figure. In between, the first and second rows of vertical lines refer to the $Nd_6Fe_{13}Si$ magnetic and nuclear contributions to the diffraction pattern. The third row refers to the Nd_2Fe_{17} contribution to the diffraction pattern.

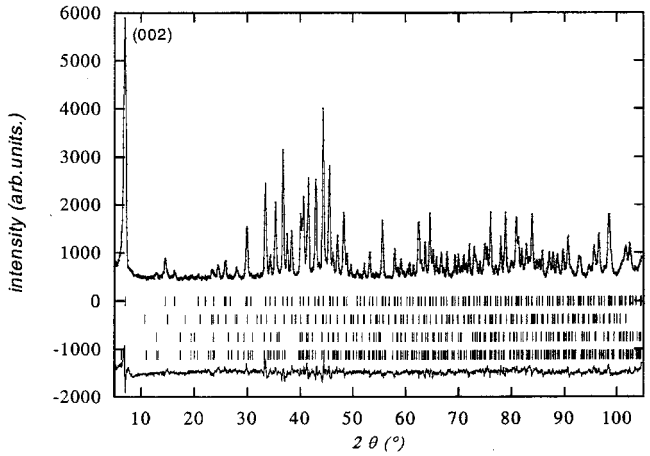

Figure 5. The powder neutron diffraction pattern of $Nd_6Fe_{13}Si$ obtained at 17 K on the MURR high resolution diffractometer with a neutron wavelength of 1.4807 Å. In the upper plot the points represent the experimental data and the full curve is the result of the Rietveld profile analysis. The difference between the experimental data and the calculated pattern is plotted on the same scale in the lowest part of the figure. In between, the first and second rows of vertical lines refer to the $Nd_6Fe_{13}Si$ magnetic and nuclear contributions to the diffraction pattern. The third and fourth rows refer to the nuclear and magnetic contributions of Nd_2Fe_{17} to the diffraction pattern.

reflection for $h + k + l = 2n$. Thus the nuclear Bravais lattice is I, whereas the magnetic Bravais lattice is I_p. Furthermore, the huge (001) intensity suggests that the main axis of antiferromagnetic ordering is confined to the (001) plane below the spin reorientation at $\sim$100 K.

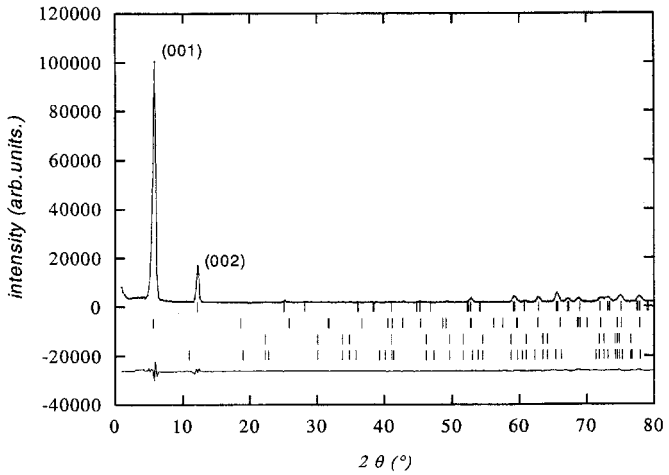

Figure 6. The powder neutron diffraction pattern of $Nd_6Fe_{13}Si$ obtained at 2 K on the D1B high flux diffractometer with a neutron wavelength of 2.52 Å. In the upper plot the points represent the experimental data and the full curve is the result of the Rietveld profile analysis. The difference between the experimental data and the calculated pattern is plotted on the same scale in the lowest part of the figure. In between, the first and second rows of vertical lines refer to the $Nd_6Fe_{13}Si$ nuclear and magnetic contributions to the diffraction pattern. The third and fourth rows refer to the nuclear and magnetic contributions of Nd_2Fe_{17} to the diffraction pattern.

Table 1. Lattice parameters and unit-cell volume of $Nd_6Fe_{13}Si$.

T (K)	a (Å)	c (Å)	V (Å^3)
2	8.016(4)	22.587(10)	1451
200	8.025(4)	22.690(10)	1461
300	8.029(4)	22.707(10)	1464
2–200 K increase	0.009	0.103	10
Increase (%)	0.11	0.46	0.66

In contrast, unlike the (001) reflection, the (003) reflection, which would be found at 19°, has either a very small or zero intensity and is unobserved within the experimental error at all temperatures between 2 and 295 K, see figure 6. Further, 94% of the magnetic scattering is contained in the low angle (001) magnetic Bragg peak. As a consequence, except for the (001) reflection observed at low angle, the neutron magnetic scattering of $Nd_6Fe_{13}Si$ shows very little dependence upon the orientation of the magnetic moments and an accurate measurement of the (001) reflection is essential in determining the magnetic structure of $Nd_6Fe_{13}Si$. Special care has been taken to reduce the beam size and adjust the beam stop in order to avoid any risk of reduction in the intensity of the low angle (001) Bragg reflection. Below the spin reorientation the presence of the (001) peak proves that the magnetic moments are aligned perpendicular to the [001] axis, i.e. within the basal plane of the tetragonal structure. From powder neutron diffraction, it is impossible to determine the orientation of the magnetic moments within the basal (a, b) plane [23]. A simple schematic of the low temperature magnetic structure (see figure 1(b)) reveals a ferromagnetic arrangement of the magnetic moments in layers of six successive sublattices, two for the neodymium sites and four for the iron sites. Each of these ferromagnetic layers is coupled antiferromagnetically with the adjacent Nd–Fe layer across the silicon layer.

Table 2. The positional parameters, isotropic thermal factors and moments in $Nd_6Fe_{13}Si$ at 17 and 295 K. The magnetic moments are within the basal plane and parallel to the *c* axis, at 17 and 295 K, respectively.

Parameter	17 K	295 K
a (Å)	8.0388(1)	8.0452(1)
c (Å)	22.709(1)	22.772(1)
Nd, 8f, z	0.1106(3)	0.1115(3)
Nd, 16l, x	0.1671(4)	0.1663(4)
Nd, 16l, y	0.6671(4)	0.6663(4)
Nd, 16l, z	0.1906(2)	0.1903(2)
Fe, 16k, x	0.0678(5)	0.0673(5)
Fe, 16k, y	0.2101(3)	0.2082(3)
Fe, $16l_1$, x	0.1777(3)	0.1783(4)
Fe, $16l_1$, y	0.6777(3)	0.6783(4)
Fe, $16l_1$, z	0.0614(2)	0.0614(2)
Fe, $16l_2$, x	0.3876(3)	0.3876(4)
Fe, $16l_2$, y	0.8876(3)	0.8878(4)
Fe, $16l_2$, z	0.0974(2)	0.0974(2)
B (Å^2) Nd	0.78(7)	1.06(8)
B (Å^2) Fe	0.70(5)	1.00(5)
B (Å^2) Si	0.70(5)	0.92(36)
μ (μ_B) Nd, 8f	3.3(2)	2.1(2)
μ (μ_B) Nd, 16l	2.9(1)	1.0(1)
μ (μ_B) Fe, 4d	2.6(1)	2.0(1)
μ (μ_B) Fe, 16k	2.5(1)	1.9(1)
μ (μ_B) Fe, $16l_1$	2.3(1)	1.8(1)
μ (μ_B) Fe, $16l_2$	1.7(1)	1.3(1)
R_p (%)	4.96	5.0
$R_{\rm exp}$ (%)	3.49	3.6
R_{wp} (%)	6.31	6.4
R_{Bragg} (%)	5.48	4.6
R_{mag} (%)	9.08	14.6

The variation in intensity of the low angle (001) Bragg peak corresponds to a change in the magnetic structure, i.e. a spin reorientation transition, which occurs at ∼100 K over a temperature range of at most 10–20 K, a narrow range which suggests a first-order transition. The hysteretic nature of the transition was not investigated by neutron diffraction. The disappearance of the (001) Bragg reflection above the spin reorientation temperature indicates that the magnetic moments are now aligned either exactly along or very close to the *c* axis of the unit cell. The Rietveld analysis of the neutron diffraction patterns, with a perfect ferromagnetic alignment of the magnetic moments along the *c* axis within a Nd–Fe layer, and with the two Nd–Fe layers adjacent to the silicon layer antiferromagnetically coupled (see figure 1(b) and table 2) gives an excellent fit. An alternate refinement of the 295 K pattern has been carried out with a tilt of the magnetic moments away from the *c* axis; the results of this refinement are given in table 3. The best fit was obtained with a very small tilt of $7^\circ \pm 3^\circ$. Similar fits of the 200 and 250 K data gave an identical tilt angle. Hence, above the spin reorientation temperature, the orientation of the magnetic moments in $Nd_6Fe_{13}Si$ is predominantly along the *c* axis of the tetragonal unit cell.

The presence of a very weak but broad peak at very low angles of $2\theta \sim 3.5^\circ$, i.e. at angles below the (001) Bragg reflection, is apparent in figure 7. This broad peak undoubtedly arises from scattering by $Nd_6Fe_{13}Si$ because, as shown in figure 7, it is not associated with the

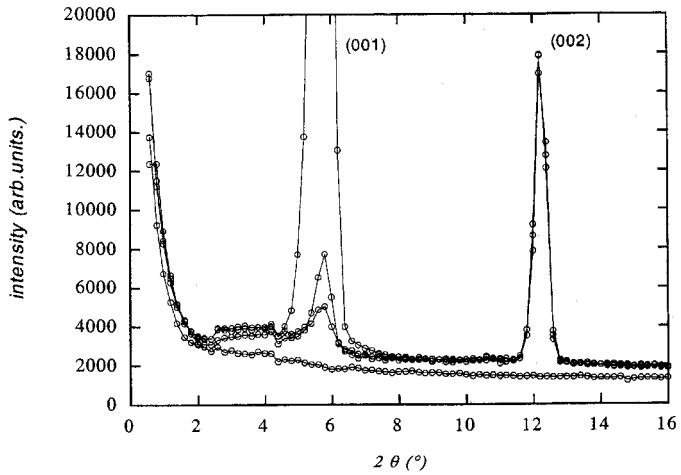

Figure 7. A comparison of the low angle neutron diffraction patterns of $Nd_6Fe_{13}Si$ obtained on D1B. From the bottom to the top, the curves refer to the empty cold cryostat, and to the $Nd_6Fe_{13}Si$ diffraction patterns obtained at 200, 130 and 2 K, respectively. Diffuse scattering is observed at $\sim$3.5° in 2θ. The increased intensity observed below $\sim$2° in 2θ is due to the direct beam. The (001) reflection at $\sim$6° in 2θ is pure magnetic scattering and the (002) reflection at $\sim$12° in 2θ is pure nuclear scattering.

Table 3. The magnetic moments in $Nd_6Fe_{13}Si$.

Parameter	2 K	50 K	100 K	150 K	200 K
μ (μ_B) Nd, 8f	3.1(5)	2.9(4)	2.4(5)	2.4(2)	2.3(3)
μ (μ_B) Nd, 16l	2.5(3)	2.4(3)	2.3(3)	1.7(2)	1.6(2)
μ (μ_B) Fe, 4d	2.8(1)	2.8(1)	2.7(1)	3.0(2)	2.9(2)
μ (μ_B) Fe, 16k	2.6(1)	2.6(1)	2.5(1)	2.9(2)	2.7(2)
μ (μ_B) Fe, $16l_1$	2.4(1)	2.4(1)	2.4(1)	2.7(2)	2.6(2)
μ (μ_B) Fe, $16l_2$	1.8(1)	1.8(1)	1.7(1)	2.0(2)	1.9(2)
θ[a] (deg)	90[a]	90[a]	90[a]	7(3)	7(2)
R_p (%)	4.56	4.33	4.50	2.31	2.15
$R_{\rm exp}$ (%)	1.75	1.75	1.78	2.00	1.99
R_{wp} (%)	6.05	5.81	6.16	3.15	2.88
R_{Bragg} (%)	7.99	6.19	7.39	3.22	3.01
R_{mag} (%)	1.84	1.68	2.13	15.5	15.1

[a] The angle between the moments and the c axis has been constrained to the given value at 2, 50 and 100 K.

cryostat. The appearance of this broad peak near the (001) reflection position may indicate the presence of short range magnetic correlations within the basal (a, b) plane, correlations which are reminiscent of and may be associated with the basal plane anisotropy observed below the spin reorientation temperature. Such diffuse scattering is often associated with a structural change. However, in $Nd_6Fe_{13}Si$ it is only of magnetic origin. The use of a two-axis spectrometer does not permit us to establish whether this diffuse scattering occurs elastically or inelastically. Further investigation is required to search for any energy transfer involved with the spin reorientation transition. In addition, the intensity of the (002) peak at 12° is totally independent of temperature from 2 to 200 K and hence results from pure nuclear scattering. Finally, the huge difference in intensity of the (001) peak at $\sim$6° is indicated in figure 7. The intensity remaining above the spin reorientation will be discussed below.

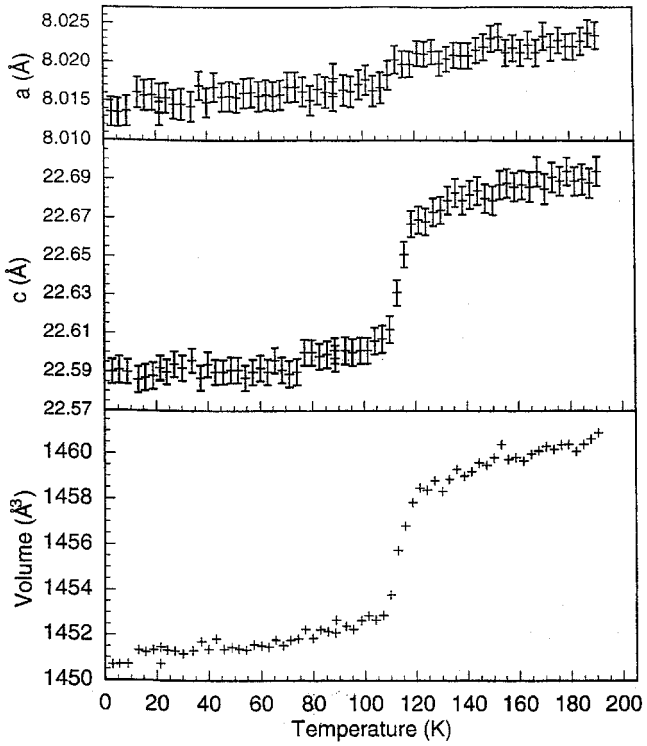

Figure 8. The temperature dependence of the *a* and *c* unit cell lattice parameters and the unit cell volume of $Nd_6Fe_{13}Si$.

Although the model proposed by Yan *et al* [13] gave a reasonable fit to the new 295 K neutron diffraction pattern reported herein, it completely fails to fit the 17 K pattern. Furthermore, the hyperfine fields measured [12, 14] in the Mössbauer spectra are significantly larger than those expected from the magnetic moments reported by Yan *et al* [13]. It is very likely that the erroneous assignment of the magnetic moment orientation [13] results from the absence of low angle (001) magnetic reflection in their neutron diffraction data. The present study benefits from a much higher resolution and a larger range of both low and high Q values in reciprocal space. Furthermore, a small amount of the Nd_2Fe_{17} secondary phase was identified in our sample of $Nd_6Fe_{13}Si$ and included in the refinements, thus improving the reliability of the final results. Yan *et al* [13] show magnetization plots that clearly indicate the presence of a ferromagnetic impurity which is probably Nd_2Fe_{17}, but they failed to include this impurity in their refinements. The amount of Nd_2Fe_{17} estimated from the Rietveld refinement is ∼6%, in reasonable agreement with the 10% found in the iron-57 Mössbauer spectra of the same sample [12, 14, 24]. However, this amount is substantially larger than the 0.5% estimated [15] from the magnetic properties. In the neutron refinements, the structural and magnetic parameters of Nd_2Fe_{17} have been constrained to those reported [1, 2, 25, 26] earlier. On the basis of the neutron diffraction and Mössbauer spectral measurements, the composition of the sample is better written as $Nd_{5.7(1)}Fe_{13.3(1)}Si_{0.92(2)}$.

Although no change in space group symmetry has been observed upon the reorientation of the magnetic moments, a significant variation in the lattice parameters, i.e. magnetostriction, is observed at the spin reorientation temperature, see figure 8. The unit cell contracts anisotropically upon cooling with a decrease of ∼0.1 and 0.5% along the *a* and *c* axes,

respectively, see table 1. This large contraction of the $Nd_6Fe_{13}Si$ unit cell volume by ∼0.66% at the spin reorientation corresponds to a substantial change [27] in spontaneous magnetostriction. A similar contraction has been observed [28] recently for $PrCo_4Ga$. The magnetostriction is also an indication of the first-order nature of the spin reorientation. A sharp increase from 1.7 to 2.3 μ_B in the neodymium 16l magnetic moment is observed at the spin reorientation. In contrast, the neodymium 8f magnetic moment increases continuously upon cooling and all the iron moments remain essentially constant upon cooling from 200 to 2 K, see table 3.

The contribution of the magnetic scattering to the overall diffraction pattern does not exceed 6% if the (001) reflection is excluded. Because of the extremely small magnetic contribution to the nuclear scattering above the spin reorientation temperature, where the (001) peak has virtually vanished, the neutron diffraction refinements have been carried out constraining the iron magnetic moments to agree with the sequence of Mössbauer hyperfine fields observed [12, 14] earlier. Consequently, the refinement of the iron magnetic moments has been carried out by constraining the ratio of the moments of the inequivalent crystallographic sites to be constant. The magnetic moments and hyperfine fields decrease in the order, $4d > 16k > 16l_1 > 16l_2$, an order which is consistent with the different iron near-neighbour environments. In the $Nd_6Fe_{13}Si$ structure, all iron sites have 12 near neighbours, but the iron 4d site has only iron near neighbours, neighbours which induce the largest magnetic moment on this site. The other iron site environments mostly differ by the number of neodymium near neighbours; the 16k site has 2 neodymium and 10 iron near neighbours, whereas the $16l_1$ and $16l_2$ sites have 3 and 5 neodymium near neighbours, respectively, among their 12 near neighbours. The influence of the nature of the near-neighbour environment on the magnitude of the iron magnetic moment in iron intermetallic compounds has been discussed extensively elsewhere [29], and the present analysis is in excellent agreement with these expectations. The quality of the neutron diffraction fits obtained with this hierarchy of magnetic moments is a further indication of the validity of the model. Finally, the weighted average iron magnetic moment of 2.3 μ_B observed in $Nd_6Fe_{13}Si$ is close to that reported [16] for $Nd_6Fe_{13}Au$ and is completely reasonable in comparison with the moments observed [1, 2, 25, 26, 30] for other iron-rich Nd–Fe binary compounds, such as Nd_2Fe_{17} and $Nd_2Fe_{14}B$, and ternary compounds, such as $Nd_2Fe_{17-x}Si_x$ and $Nd_2Fe_{14-x}Si_xB$.

The 2 K neodymium magnetic moments are 3.1 and 2.5 μ_B for the 8f and 16l sites, respectively, and are close to the Nd^{3+} free ion value of 3.27 μ_B. As indicated in table 2, the error for the neodymium magnetic moment is larger for the 8f than for the 16l site as a result of their differing multiplicities, multiplicities which lead to different refinement sensitivities. The neodymium magnetic moments are found to be much more sensitive to changes in temperature than are the iron moments and a significant decrease in their magnitude is observed near the spin reorientation temperature, see table 3. The difference between the two neodymium site magnetic moments extends to their thermal dependencies and results in a difference of ∼1 μ_B at 295 K. This difference probably originates from the different environments of the two neodymium sites. Whereas the neodymium 8f site has twelve iron, four neodymium and one silicon near neighbours, the 16l site has ten neodymium, four iron, and two silicon near neighbours. Hence the twelve iron near neighbours of the neodymium 8f site induce a larger magnetic moment and stronger exchange interactions at all temperatures.

4. Mössbauer spectral results

Because our earlier Mössbauer spectral study [12] was limited to between 80 and 295 K, the Mössbauer spectra of $Nd_6Fe_{13}Si$ have been measured between 4.2 and 135 K and are shown in figure 9. The spectra obtained at 135, 100 and 80 K are virtually identical to those reported

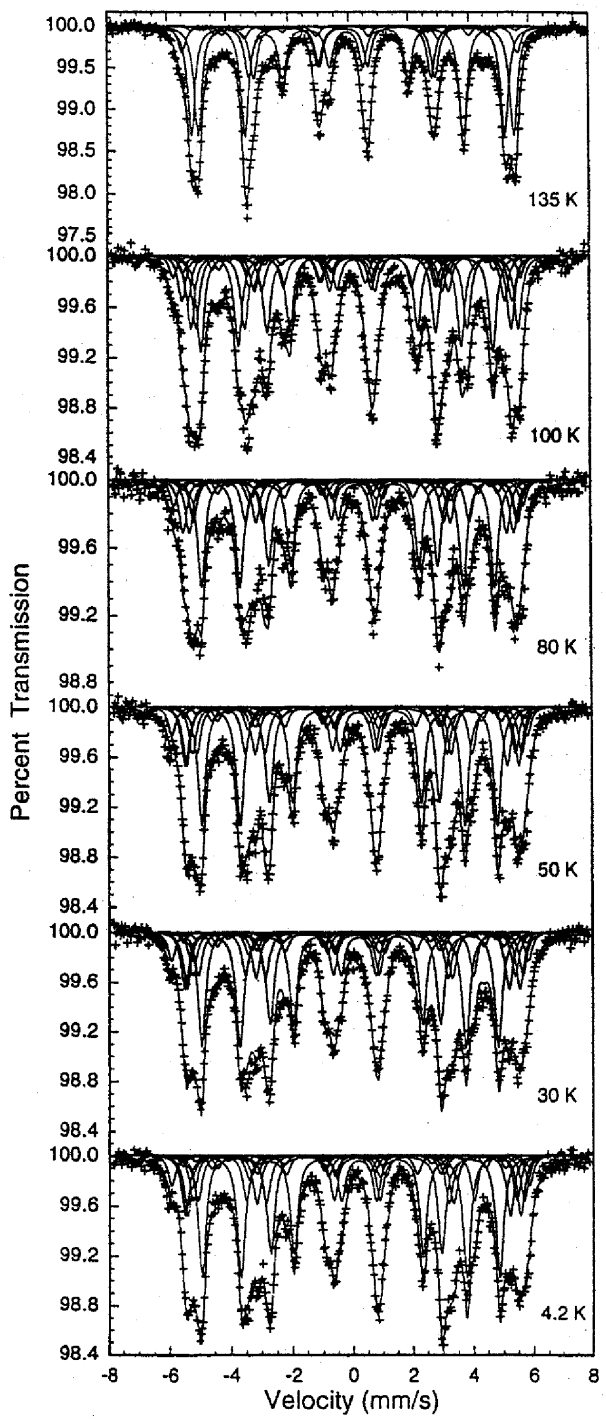

Figure 9. The Mössbauer spectra of $Nd_6Fe_{13}Si$ obtained at the indicated temperatures.

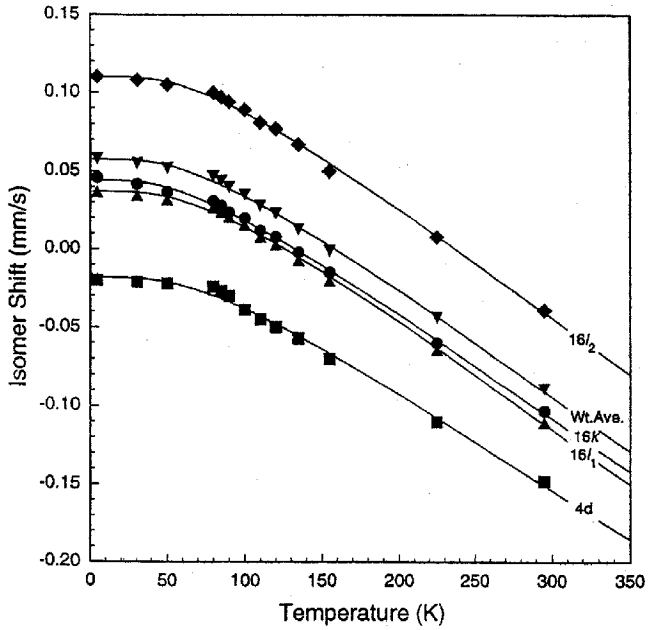

Figure 10. The temperature dependence of the Mössbauer spectral isomer shifts observed for $Nd_6Fe_{13}Si$. The data is fitted with a Debye model of the second-order Doppler shift. The error bars are smaller than the size of the data points.

earlier [12] and it is apparent from figure 9 that there is very little change in the Mössbauer spectra between 80 and 4.2 K, i.e. as might be expected from the neutron diffraction results reported above, the major changes in the Mössbauer spectra occur between 110 and 80 K. As a consequence of the similarity below 80 K, the spectra have been fitted with the same model we used earlier [12], and the resulting hyperfine parameters are given in table 4. In contrast to expectation, a superposition of both axial and basal components is observed below 130 K and will be discussed below.

The temperature dependence of the four different isomer shifts, and their weighted average, is shown in figure 10. The higher temperature data in this and subsequent figures have been taken from our earlier paper [12]. The fits shown in this figure correspond to the Debye model of the second-order Doppler shift [31] and the resulting parameters are given in table 5. The observed effective vibrating masses, M_{eff}, of the iron-57 nuclide range from 57 to 64 g mol^{-1} with an accuracy of ± 2 g mol^{-1}; the increase above 57 g mol^{-1} is that expected from the covalency of the iron bonding in $Nd_6Fe_{13}Si$. The resulting effective Mössbauer temperatures, θ_M, the equivalent of the Debye temperature, range from 239 to 278 K, with an accuracy of ± 5 K, and are typical of the values found for similar intermetallic compounds [24].

The temperature dependence of the site average hyperfine field observed in $Nd_6Fe_{13}Si$, and their weighted average, is shown in figure 11. There is no significant change in any of the hyperfine fields at the spin reorientation in agreement with the smooth temperature dependence of the iron magnetic moments obtained from the neutron diffraction studies, see table 3. The sequence of decreasing hyperfine fields is the same as that observed [12] in $Nd_6Fe_{13}X$, where X is Cu, Ag, Au, In, Tl, Ge, Sn, Pb, Sb and Bi, a sequence which is the same in compounds with both axial and basal magnetizations. In general it is found [12] that the $Nd_6Fe_{13}X$ compounds with axial magnetizations have somewhat higher hyperfine fields.

Table 4. The Mössbauer spectral hyperfine parameters[a] for $Nd_6Fe_{13}Si$. (Note: The linewidths are 0.30 mm s^{-1} at 4.2, 30, 50, 80, 90 and 110 K, and 0.34 mm s^{-1} at 295 K.)

		Axial						Basal						
Parameter	T (K)	4d	16k	$16l_1$	$16l_2$	W. av.	% A	4d	16k	16k′	$16l_1$	$16l_2$	W. av.	% A
H (kOe)	295	289	277	257	187	244	100	—	—	—	—	—	—	0
	110	345	333	319	226	297	49	352	329	323	294	225	287	51
	90	347	335	320	231	299	28	361	336	325	300	229	292	72
	80	347	334	322	230	299	25	361	336	326	300	228	292	75
	50	349	336	325	232	302	25	363	339	329	302	229	294	75
	30	350	337	323	233	302	24	364	340	331	303	230	295	76
	4.2	352	338	325	233	303	24	365	340	331	304	230	296	76
δ[a] (mm s^{-1})	295	−0.148	−0.103	−0.110	−0.039	−0.089	100	—	—	—	—	—	—	0
	110	−0.045	0.012	0.008	0.081	0.028	49	−0.045	0.012	0.012	0.008	0.081	0.028	51
	90	−0.030	0.024	0.021	0.094	0.040	28	−0.030	0.024	0.024	0.021	0.094	0.040	72
	80	−0.024	0.031	0.027	0.100	0.047	25	−0.024	0.031	0.031	0.027	0.100	0.047	75
	50	−0.022	0.037	0.032	0.105	0.052	25	−0.022	0.037	0.037	0.032	0.105	0.052	75
	30	−0.021	0.042	0.035	0.108	0.055	24	−0.021	0.042	0.042	0.035	0.108	0.055	76
	4.2	−0.020	0.046	0.037	0.110	0.058	24	−0.020	0.046	0.046	0.037	0.110	0.058	76
QS (mm s^{-1})	295	0.28	0.35	0.30	0.28	—	100	—	—	—	—	—	—	0
	110	0.28	0.36	0.30	0.29	—	49	−0.040	0.060	−0.038	−0.135	−0.131	—	51
	90	0.28	0.36	0.30	0.29	—	28	−0.040	0.060	−0.038	−0.146	−0.140	—	72
	80	0.28	0.36	0.30	0.29	—	25	−0.040	0.060	−0.038	−0.148	−0.134	—	75
	50	0.28	0.36	0.30	0.29	—	25	−0.040	0.060	−0.038	−0.143	−0.154	—	75
	30	0.28	0.36	0.30	0.29	—	24	−0.040	0.060	−0.038	−0.151	−0.156	—	76
	4.2	0.28	0.36	0.30	0.29	—	24	−0.040	0.060	−0.038	−0.149	−0.137	—	76

[a] Relative to α-iron foil at room temperature.

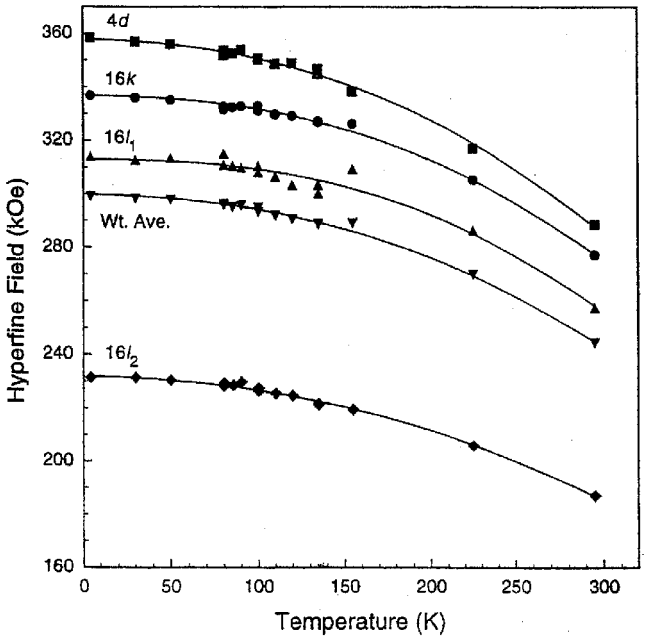

Figure 11. The temperature dependence of the site average hyperfine fields, and their weighted average, for $Nd_6Fe_{13}Si$. The full curves are a guide to the eye and the error bars are smaller than the size of the data points.

Table 5. Derived Mössbauer parameters in $Nd_6Fe_{13}Si$.

Parameter	4d	16k	$16l_1$	$16l_2$	Wt av
M_{eff} (g mol^{-1})	64	60	57	57	58
θ_M (K)	277	239	278	270	267
δ_o (mm s^{-1})	0.050	0.106	0.113	0.184	0.129
μ^a (μ_B)	2.8	2.6	2.4	1.8	—
μ^b (μ_B)	2.5	2.3	2.1	1.6	—

[a] The 2 K iron magnetic moments obtained by neutron diffraction.
[b] The 4.2 K iron magnetic moments obtained from the Mössbauer spectra.

The iron magnetic moments measured at 2 K by neutron diffraction and calculated from the 4.2 K hyperfine fields using the conversion factor of 145 kOe μ_B^{-1}, see table 5, are in very good agreement when one considers that the hyperfine fields include the dipolar contribution, which is not included in the neutron diffraction values. The ratio of the hyperfine field to the neutron measured magnetic moment is 128 ± 2 kOe μ_B^{-1}, a value which is somewhat low but not unreasonable for an intermetallic compound and indicates the enhanced sensitivity of the hyperfine field to the orbital contribution of the moment.

The reduced weighted average hyperfine field versus the reduced temperature for $Nd_6Fe_{13}Si$ is shown in figure 12. The 4.2 K weighted average hyperfine field of 299 kOe and the Néel temperature of 411 K were used to calculate the reduced values in this figure. For a reduced temperature below 0.3, the reduced weighted average field follows the Brillouin curve for spin 5/2, as would be expected for the average iron magnetic moment of 2.3 μ_B observed at 2 K by neutron diffraction. Above a reduced temperature of 0.3, i.e. above the spin reorientation temperature, the weighted average hyperfine field is larger

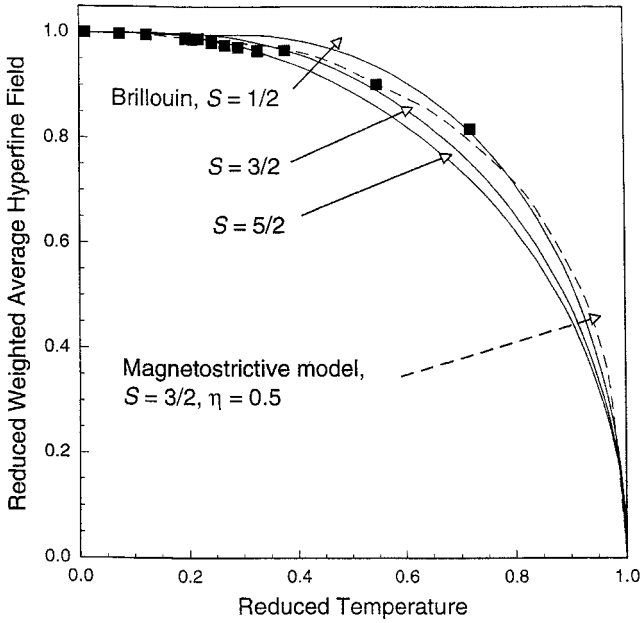

Figure 12. The reduced weighted average hyperfine field, relative to 299 kOe, versus the reduced temperature, relative to 411 K, for $Nd_6Fe_{13}Si$. The three full curves are the Brillouin function for spin 5/2, lower, 3/2 and 1/2. The broken curve is the curve calculated [32] for spin 3/2 and $\eta = 0.5$.

than expected from the Brillouin curve and follows the temperature dependence calculated from the magnetostrictive model of Bean and Rodbell [32], calculated for a spin 3/2 and a magnetostrictive factor, η, of 0.5. The existence of magnetostriction in $Nd_6Fe_{13}Si$ is supported by magnetostriction measurements [27] and the substantial unit-cell volume change occurring at the spin reorientation temperature as observed by neutron diffraction, see section 3 and figure 8.

The temperature dependence of the percentage of the axial and basal contributions to the Mössbauer spectra of $Nd_6Fe_{13}Si$ (see figure 13) is an extension of figure 9 in our earlier work [12] from 80 to 4.2 K. Contrary to all expectations, the percentage of the axial and basal contribution did not saturate at 0 and 100%, respectively, at 4.2 K. Rather, these percentages are essentially constant at 25 and 75%, respectively, between 4.2 and 80 K. A careful study of the Mössbauer spectra indicates that there is no possibility that the 4.2 K spectrum could be fitted with only five sextets, as is observed for the $Nd_6Fe_{13}X$ compounds, where X is Cu, Ag and Au, which exhibit strictly basal magnetization, or as might be expected, if the iron magnetic moments were canted from the *c* axis. However, the four axial and five basal sextets used in the fits shown in figure 9 agree completely with the sextets observed in the axial $Nd_6Fe_{13}Sn$ compound [33] and in the basal $Nd_6Fe_{13}X$ compounds [12], where X is Cu, Ag and Au. Hence, from the analysis of the Mössbauer spectra of $Nd_6Fe_{13}Si$, we conclude that the spin reorientation occurs in only 75% of the sample.

The hysteretic nature of the spin reorientation was not systematically investigated by Mössbauer spectroscopy. However, two separate experimental studies between 4.2 and 100 K and between 80 and 295 K give identical percentages for the axial and basal contributions to the spectra obtained between 80 and 100 K. If there is any thermal hysteresis present it is less than 10 degrees.

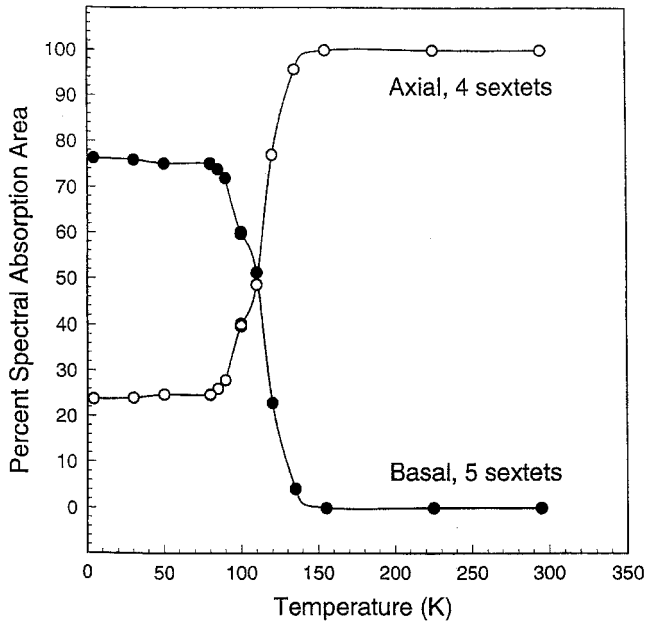

Figure 13. The temperature dependence of the percentage of the axial and basal contributions to the Mössbauer spectra of $Nd_6Fe_{13}Si$.

5. Discussion

Because of the above analysis of the Mössbauer spectra in terms of a mixed magnetic phase, refinements of the 17 K neutron diffraction pattern of $Nd_6Fe_{13}Si$ were refitted with a model in which 75% of the sample exhibit basal magnetization and 25% exhibit axial magnetization; these refits were virtually identical to those obtained with the basal model described above and in figure 1(b) and table 2. The same conclusion has been drawn from the analysis of the 2 or 10 K neutron diffraction data; the fits using the mixed 75% basal and 25% axial magnetic phases were slightly better than the 100% basal phase. Thus, below the spin reorientation temperature, the neutron powder diffraction patterns are completely compatible with magnetic moments either oriented within the basal plane or with a mixed magnetic phase.

The mixed magnetic phase would initially seem rather unlikely because the $Nd_6Fe_{13}Si$ phase is very homogeneous, as is indicated by the narrow diffraction peaks observed in both the x-ray and neutron powder diffraction patterns and the narrow linewidths observed in the Mössbauer spectra. Further, because the spin reorientation transition exhibits first-order characteristics, as is indicated by the squareness of the thermal evolution of the intensity of the (001) Bragg peak, see figure 3, the step-like temperature dependence of the c lattice parameter and of the unit-cell volume, see figure 8, and the sharp peak in the thermal expansion coefficient [27], the percentages of axial and basal phase observed may depend on the cooling procedure and cycle. The possibility of supercooling of the axial phase is not excluded by our neutron diffraction studies. However, the Mössbauer spectral studies require many days at low temperature and hence it would appear that, if supercooling exists, it must persist for many days, a persistence which seems unlikely. Alternatively, the presence of the secondary ferromagnetic phase of Nd_2Fe_{17} in the sample may be responsible for the observed mixed magnetic phase. Indeed, at low temperature the magnetic field developed by the Nd_2Fe_{17} grains will induce [16] a net magnetization in a direction perpendicular to the preferred basal

moment direction, as is commonly observed in antiferromagnets. In other words, the grains of $Nd_6Fe_{13}Si$, which are in the neighbourhood of the Nd_2Fe_{17} grains, will orient their magnetic moments parallel to the *c* axis although the preferred moment direction is perpendicular to the *c* axis. Those grains which are unaffected by the Nd_2Fe_{17} will, of course, show the observed first-order spin reorientation. Finally, the existence of a mixed magnetic phase at about 100 K is in complete agreement with the zero magnetostriction measured [27] at 115 K.

6. Conclusions

Neutron diffraction results indicate that the magnetic structure of $Nd_6Fe_{13}Si$ is characterized by Nd–Fe ferromagnetic layers which are antiferromagnetically coupled across the intervening silicon layers. The antiferromagnetic order is due to the exchange interactions between the neodymium-rich layers, interactions that are mediated by the silicon-containing layer. This magnetic structure differs significantly from the one proposed by Yan *et al* [13], a structure in which there were antiferromagnetic interactions within the iron layers. Further, unlike the observation of Yan *et al* [13], no compensation temperature has been observed in $Nd_6Fe_{13}Si$.

The thermal evolution of both the neutron diffraction patterns and the Mössbauer spectra has revealed a spin reorientation at $\sim$100 K. In the neutron diffraction pattern, the signature of this spin reorientation is predominantly the huge increase in intensity of the (001) diffraction peak at 6.4°. The observation of this increase at such a small diffraction angle was only possible through extremely careful intensity measurements with the high resolution D1b neutron diffractometer.

Above 100 K, the magnetic moments of the $Nd_6Fe_{13}Si$ phase are along the *c* axis of the structure, whereas below 100 K they are mainly found within the basal plane. The spin reorientation transition is first order as indicated by the accompanying large anisotropic change in the unit-cell volume and the squareness of the thermal evolution of the magnetic neutron scattering intensity of the (001) peak. The anisotropic lattice changes reveal a change in the magnetoelastic coupling involved in this compound.

Finally, the coexistence of basal and axial magnetic orientations, even at 4.2 K, as is indicated by the Mössbauer spectra, can be explained by the influence of the magnetic field of the ferromagnetic Nd_2Fe_{17} secondary phase on the orientation of the magnetic moments of the neighbouring antiferromagnetic $Nd_6Fe_{13}Si$ phase.

Acknowledgments

The authors would like to thank Drs C H de Groot and F R de Boer for providing the sample, Dr W B Yelon for help in obtaining the high-resolution neutron diffraction data, Dr O A Pringle for help in the preliminary fit of this data, and Drs P Schobinger-Papamantellos and F Hatert for interesting discussions during the course of this work. OI thanks the Centre National de la Recherche Scientifique, CNRS, France for grant action initiative No 7418. The authors are grateful to the Institut Laue Langevin and the CNRS for the use of the high flux powder diffractometer D1B and to the Missouri Research Reactor for the neutron diffraction experiments performed on the high resolution instrument. GJL thanks the US National Science Foundation for grants DMR95-21739 and INT-9815138.

References

[1] Long G J, Marasinghe G K, Mishra S, Pringle O A, Grandjean F, Yelon W B, Pourarian F and Isnard O 1993 *Solid State Commun.* **88** 761
[2] Artigas M, Fruchart D, Isnard O, Miraglia S and Soubeyroux J L 1999 *J. Alloys Compounds* **291** 282
[3] Isnard O and Buschow K H J 1997 *J. Alloys Compounds* **267** 50

[4] Buschow K H J 1988 *J. Appl. Phys.* **63** 3130
[5] Solzi M, Pareti L, Moze O and David W I F 1988 *J. Appl. Phys.* **64** 5084
[6] Allemand J, Letant A, Moreau J M, Nozières J P and Perrier de la Bâthie R 1990 *J. Less-Common Met.* **166** 73
[7] Weitzer F and Rogl P 1990 *J. Less-Common Met.* **167** 135
[8] Klesnar H and Rogl P 1991 *J. Mater. Res.* **6** 53
[9] Weitzer F, Leithe-Jasper A, Rogl P, Hiebl K, Rainbacher A, Wiesinger G, Steiner W, Friedl J and Wagner F E 1995 *J. Appl. Phys.* **75** 7745
[10] Kajitani T, Nagayama K and Umeda T 1992 *J. Magn. Magn. Mater.* **117** 379
[11] Nozières J P 1990 *PhD Thesis* University of Grenoble
[12] Hautot D, Long G J, Grandjean F, de Groot C H and Buschow K H J 1998 *J. Appl. Phys.* **83** 1554
[13] Yan Q W, Zhang P L, Sun X D, Hu B P, Wang Y Z, Rao X L, Liu G C, Gou C, Chen D F and Cheng Y F 1994 *J. Phys.: Condens. Matter* **6** 3101
[14] Hautot D, Long G J, Grandjean F, de Groot C H and Buschow K H J 1997 *J. Appl. Phys.* **81** 5435
[15] de Groot C H and de Boer F R 1998 *Phys. Rev.* B **57** 11472
[16] Schobinger-Papamantellos P, Buschow K H J, de Groot C H, de Boer F R, Boettger G and Ritter C 1999 *J. Phys.: Condens. Matter* **11** 4469
[17] Schobinger-Papamantellos P, Buschow K H J, de Groot C H, de Boer F R, Ritter C, Fauth F and Boettger G 1998 *J. Alloys Compounds* **280** 44
[18] Opechowski W and Guccione R 1965 *Magnetism* vol IIA, ed G T Rado and H Shul (London: Academic) p 105
[19] Schobinger-Papamantellos P, Buschow K H J, de Groot C H, de Boer F R and Ritter C 2000 *J. Magn. Magn. Mater.* **218** 31
[20] McCusker L B, Von Dreele R B, Cox D E, Louër D and Scardi P 1999 *J. Appl. Crystallogr.* **32** 36
Rodriguez-Carvajal J 1993 *Physica* B **192** 55
[21] Sears V F 1992 *Neutrons News* **3** 26
[22] Hautot D and Long G J 1999 unpublished data
[23] Shirane G 1952 *Acta Crystallogr.* **12** 282
[24] Hautot D 2000 *PhD Thesis* University of Missouri-Rolla
[25] Isnard O, Miraglia S, Soubeyroux J L, Fruchart D and Stergiou A 1990 *J. Less-Common Met.* **162** 273
[26] Isnard O, Miraglia S, Soubeyroux J L and Fruchart D 1992 *Solid State Commun.* **87** 13
[27] Tajabor N, Alinejad M R and Pourarian F 2002 *Physica* B **321** 60
[28] Zlotea C and Isnard O 2003 *J. Alloys Compounds* **346** 29
[29] Isnard O and Fruchart D 1994 *J. Alloys Compounds* **205** 1
[30] Chacon C and Isnard O 2000 *J. Appl. Phys.* **88** 2342
[31] Long G J, Hautot D, Grandjean F, Morelli D T and Meisner G P 1999 *Phys. Rev.* B **60** 7410
[32] Bean C P and Rodbell D S 1962 *Phys. Rev.* **126** 104
[33] Weitzer F, Leithe-Jasper A, Rogl P, Hiebl K, Noël H, Wiesinger G and Steiner W 1993 *J. Solid State Chem.* **104** 368